

Preparation of ZnO-Coated LiV_3O_8 as Cathode Materials for Rechargeable Lithium Batteries

Xiao-Yu Cao*, Li-Jing Guo, Jian-Ping Liu, Ling-Ling Xie

School of Chemistry and Chemical Engineering, Henan University of Technology,
Zhengzhou 450001 China

*E-mail: caoxy@haut.edu.cn

Received: 8 November 2010 / Accepted: 20 January 2011 / Published: 1 February 2011

The layered LiV_3O_8 and different weight ratios of ZnO-coated LiV_3O_8 samples were synthesized as cathode materials for rechargeable lithium batteries via a facile low temperature method. The as-prepared samples were characterized by XRD, SEM, and the galvanostatic discharge-charge techniques. It is found that the 2 wt.% ZnO-coated LiV_3O_8 sample exhibits less capacity loss during long-term cycling than pristine one. The 2 wt.% ZnO-coated LiV_3O_8 sample displays the initial discharge capacity of 274.2 mAh g^{-1} in the range of 4.0~1.8 V at a current rate of 30 mA g^{-1} and maintains a stable discharge capacity of 240.9 mAh g^{-1} after 44 cycles. Moreover, the crucial role that ZnO-coating plays in ameliorating the cycleability of LiV_3O_8 has been described.

Keywords: LiV_3O_8 , cathode, ZnO-coating, rechargeable lithium battery

1. INTRODUCTION

LiV_3O_8 with the layered structure has received great attention as an excellent potential cathode material for rechargeable lithium batteries because of its easy preparation, high energy density, and low cost [1–4]. However, it is well known that the preparation methods for LiV_3O_8 strongly affect its electrochemical properties. Therefore, great efforts have been paid on exploring the novel synthesis and post-processing methods for LiV_3O_8 in the past two years [3,4,7–14]. To date, the synthesis of LiV_3O_8 generally involves two categories of method. One is the high temperature solid state synthesis (HT-SSS) method by employing Lithium salts and vanadium oxides as the raw materials; the other is the soft-chemical synthesis (SCS) methods which are carried out under much milder condition owing to mixing the reactants at the atomic scale or preparing the precursors constituted of ultra-fine particles. The former requires high reaction temperature ($680 \text{ }^\circ\text{C}$) [15], and the morphologies of the resulting

powders are usually large irregular particles. As a result, the HT-SSS powder only delivers a low discharge capacity of about 180 mAh g⁻¹. In contrast, the latter only needs lower calcination temperature and shorter calcination time, and thereby results in the controllable size and peculiar morphologies such as nanorods [1,5,10–13], nanospheres [6,10], nanoflasks [8], nanoflowers [9] and nanoneedles [14], which significantly improves the discharge capacity of over 300 mAh g⁻¹.

However, it is a fact that the cycleability of some SCS-derived LiV₃O₈ powders is not as good as desired, which restricts its application in rechargeable lithium batteries. In order to address this problem, many researchers have intensively investigated Li_{1-x}M_xV₃O₈ (M=Ag) [15], LiM_xV_{3-x}M_xO₈ (M=Ni, Mn) [17,18], M_xLiV₃O₈ (M=Y, Si, Cu, Cr, and B) [19–24], and LiV₃O_{8-x}M_x (M=F, Cl) [25–26] to attain stable capacity retention of LiV₃O₈ by substituting the different doping elements for Li, V, and O. Recently, Jiao et al. [27] investigated the effect of AlPO₄ nanowire coating on the electrochemical performance of LiV₃O₈, indicating that the surface coating is an effect modification technique for improve the cycleability of LiV₃O₈. However, to the best of our knowledge, attempt to coat the electrochemically inactive oxide on the LiV₃O₈ electrode is still rare.

In this work, we have synthesized LiV₃O₈ and ZnO-coated LiV₃O₈ materials through the rheological phase reaction method. The effect of ZnO coating on the electrochemical properties of LiV₃O₈ was investigated in detail.

2. EXPERIMENTAL

LiV₃O₈ powders were prepared by the rheological phase reaction method. Firstly, stoichiometric amounts of LiOH·H₂O and NH₄VO₃ were mixed thoroughly by grinding in an agate mortar. Secondly, the solid–liquid rheological body (muddy state) was obtained by adding a proper amount of distilled water dropwise. Then the rheological body was transferred to a cylindrical Teflon-lined stainless autoclave. Thirdly, the sealed autoclave was heated in an air circulation thermostatic drier (101-OEBS, Beijing Yongguangming Medical Instrument, China) at 90 °C for 5 h and then dried at 120 °C for 8 h. Afterwards, the resulting precursor was obtained by grinding the air-dried rheological body. Finally, a corundum crucible as container, the precursor was heated in CMF-1100X muffle furnace (Zhengzhou Kejing Technology Co., Ltd, Chian) in air at 300 °C for 10 h to get the final LiV₃O₈ powder. The modification with ZnO involved the dispersion of the as-prepared LiV₃O₈ in an ethyl-alcohol solution of Zn(CH₃CO₂)₂·2H₂O. After the evaporation of the solvent at 80 °C, the obtained powder was calcined at 350 °C for 5 h to obtain ZnO-coated LiV₃O₈ materials.

XRD analysis was carried out on an XRD-6000 diffractometer (Shimadzu, Japan) with Cu K α radiation ($\lambda = 1.54056 \text{ \AA}$). SEM images of the as-prepared powders were taken on a JSM-6510LV Scanning electron microscope (JEOL, Japan). The cathode films were composed of the as-synthesized active powders, acetylene black (AB) and polytetrafluoroethylene (PTFE) binder at a weight ratio of 8:1:1. Then the working electrodes were fabricated by loading the cutting disc films into the stainless-steel meshes and they were subjected to a pressure of 10 MPa. Lithium foil (Wuhan Newthree Technology Co., Ltd, China) was used as counter-electrode and the commercial polyethylene (PE) film (ND420 H129-100, Asahi Kasei Chemical Co., Japan) was used as separator. The electrolyte was a

solution of 1 mol dm^{-3} LiClO_4 dissolving in the 1:1 mixture of ethylene carbonate and dimethyl carbonate (Zhangjiagang Guotai-Huarong New Chemical Materials Co., Ltd, China). The CR2016 type coin cells were assembled in a high purified argon-filled dry box, where the coin cell case is stainless-steel and purchased from Shenzhen Meisen Machine-electro Equipment Co., Ltd, China. All the coin cells were tested on a multi-channel CT-3008W-5V5mA-S₄ battery tester (Shenzhen Neware Technology Co., Ltd, China) at 25 °C. Discharge/charge cycles were carried out at the 30 mA g^{-1} rate over a potential range between 1.8 and 4.0 V.

3. RESULTS AND DISCUSSION

Fig. 1 presents the XRD patterns of the pristine LiV_3O_8 and 1, 2, 3 wt.% ZnO-coated samples, respectively. As shown in Fig. 1, the diffraction patterns of all the samples conform to the monoclinic system with space group $P2_1/m$. The main peaks for the samples are labeled with miller indices. The absence of diffraction patterns of ZnO may be due to its very low content and amorphous structure. In addition, it is found that the (100) diffraction peak of the pristine LiV_3O_8 is much weaker than those of ZnO-coated ones, which should be ascribed to the secondary calcination during the heat treatment process at 350 °C for 5 h.

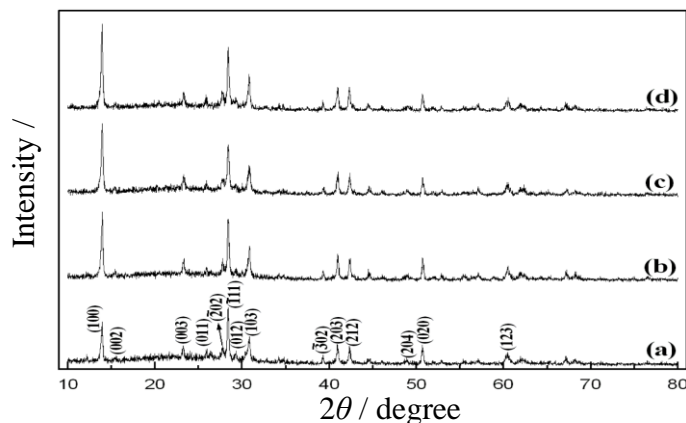


Figure 1. XRD patterns of (a) pristine LiV_3O_8 , (b) 1 wt.% ZnO-coated LiV_3O_8 , (c) 2 wt.% ZnO-coated LiV_3O_8 , and (d) 3 wt.% ZnO-coated LiV_3O_8 samples.

Fig. 2 shows the surface morphologies of the as-synthesized LiV_3O_8 and the ZnO-coated LiV_3O_8 by SEM obtained at the magnification 10, 000 \times . In the case of the pristine LiV_3O_8 material, the particles are found to be crystalline with the agglomeration. For the sample treated with 1 wt.% of ZnO, it displays a dispersed strip-like particles and a bright ZnO grains are developed on the its surfaces. With the content of ZnO heightening, the ZnO particles coverage on the surface of LiV_3O_8 gradually increases. Based on the results of XRD and SEM, it could be confirmed that the ZnO particles is only covered on the surface of LiV_3O_8 and do not modify the layered structure of LiV_3O_8 under such a preparation condition.

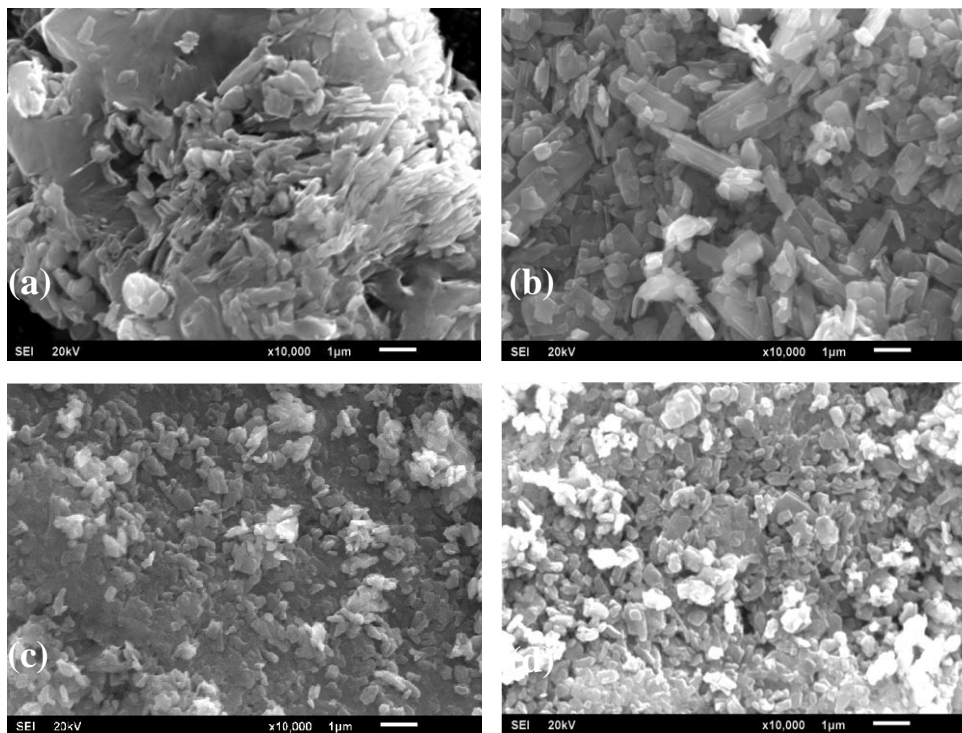


Figure 2. SEM images of (a) pristine LiV_3O_8 , (b) 1 wt.% ZnO-coated LiV_3O_8 , (c) 2 wt.% ZnO-coated LiV_3O_8 , and (d) 3 wt.% ZnO-coated LiV_3O_8 samples.

Fig. 3 shows the initial discharge/charge curves of the pristine LiV_3O_8 and 1, 2, 3 wt.% ZnO-coated LiV_3O_8 samples. It can be seen that the pristine LiV_3O_8 demonstrates the initial discharge/charge capacities of $310.67/309.9 \text{ mAh g}^{-1}$, whereas the initial discharge/charge capacities of the 1, 2, 3 wt.% ZnO-coated LiV_3O_8 samples amount to $281.5/274.1$, $274.2/280.1$, and $271/276.2 \text{ mAh g}^{-1}$, respectively.

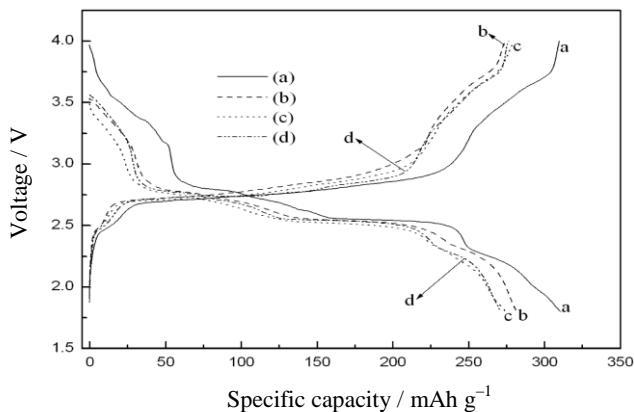


Figure 3. The initial discharge curves of (a) pristine LiV_3O_8 , (b) 1wt.% ZnO-coated LiV_3O_8 , (c) 2wt.% ZnO-coated LiV_3O_8 , and (d) 3wt.% ZnO-coated LiV_3O_8 samples.

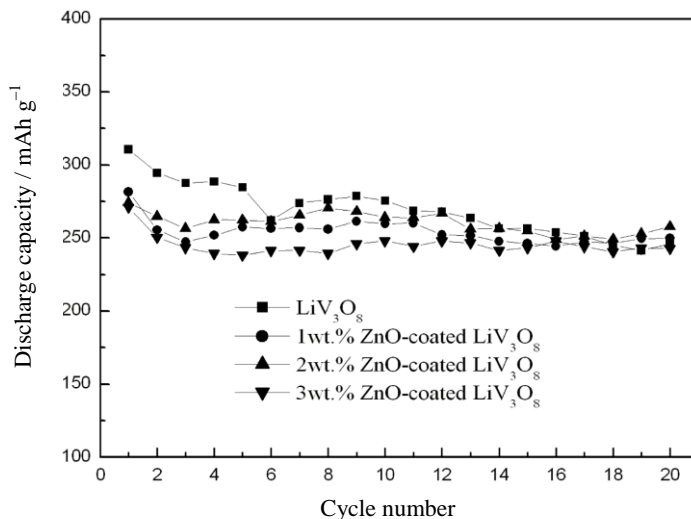


Figure 4. Discharge capacity vs. cycle number curves of pristine LiV_3O_8 and ZnO-coated LiV_3O_8 samples.

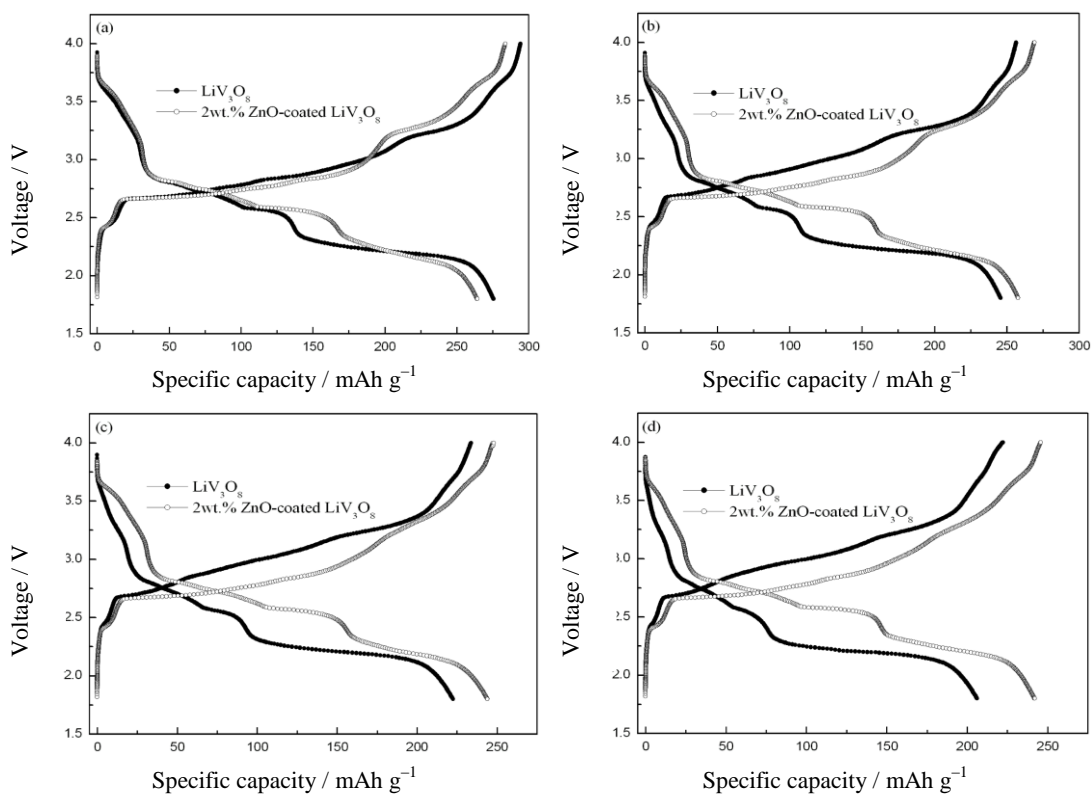


Figure 5. The selected discharge/charge curves of pristine LiV_3O_8 and 2 wt.% ZnO-coated LiV_3O_8 samples at different cycles (a) 10th cycle, (b) 20th cycle, (c) 30th cycle, (d) 40th cycle.

The initial discharge/charge capacities of the ZnO-coated LiV_3O_8 samples are slightly lower in all cases than that of the pristine LiV_3O_8 sample. The lower initial discharge/charge capacities of the ZnO-coated LiV_3O_8 may be the result of the introducing ZnO to the surface of LiV_3O_8 particle because ZnO is electrochemically inactive and counted in the quality of the overall active electrode material.

The cycling performance of the pristine LiV_3O_8 and ZnO-coated LiV_3O_8 samples for the first twenties cycles are shown in Fig. 4. As shown in Fig. 4, the capacity retention of the ZnO-coated LiV_3O_8 samples is improved compared to the pristine LiV_3O_8 sample. The pristine LiV_3O_8 sample displays a 20.89% of capacity loss after 20 cycles, whereas only 11.23%, 5.98% and 10.41% of capacity loss is observed for the 1, 2, 3 wt.% ZnO-coated LiV_3O_8 samples though they all manifest a little lower initial discharge capacity. Among these ZnO-coated LiV_3O_8 samples, the 2 wt.% ZnO-coated LiV_3O_8 sample exhibits the best cycling performance. However, the discharge capacity (242.8 mAh g^{-1}) of 3 wt.% ZnO-coated LiV_3O_8 sample at the 20th cycle is less than that (245.8 mAh g^{-1}) of the pristine LiV_3O_8 sample at the same cycle, indicating that the suitable amount of ZnO coating is essential for improving the electrochemical properties of LiV_3O_8 .

The discharge/charge curves of the 10th, 20th, 30th, and 40th cycles for the pristine LiV_3O_8 and 2 wt.% ZnO-coated LiV_3O_8 samples are illustrated in Fig. 5. According to Fig. 5, there are several charge/discharge platforms in the voltage curves whose shapes are similar to each other, which correspond to the Li^+ intercalation/deintercalation in the $[\text{V}_3\text{O}_8]$ layers. With respect to the 10th cycle in Fig. 5(a), the 2 wt.% ZnO-coated LiV_3O_8 exhibits lower discharge plateaus and higher charge plateaus compared with the pristine LiV_3O_8 . However, the 2 wt.% ZnO-coated LiV_3O_8 displays much higher discharge platforms, lower charge platforms and higher charge/discharge capacities than those of the pristine LiV_3O_8 with the further cycling, suggesting that the 2 wt.% ZnO-coated LiV_3O_8 undergoes a decreased electrode polarization after a few cycles.

Fig. 6 shows the differential capacity curves of the pristine LiV_3O_8 and 2 wt.% ZnO-coated LiV_3O_8 samples calculated from the 10th, 20th, 30th and 40th charge-discharge curves, which emphasizes the details of the voltage curves and provides a more realistic explanation for the actual state of the cathode material under the galvanostatic cycling [28]. The peaks in the curve correspond to the phase transitions during the Li^+ intercalation/deintercalation in $[\text{V}_3\text{O}_8]$ layers. In the case of the pristine LiV_3O_8 sample, there are six pairs of redox peaks (P1→P6 and P'1→P'6) in the curves, where the oxidation peak relative to the reduction peak P3 is splitted into two peaks P'3 and P'3'. In addition, the excessive movements of the redox peaks and fadeouts of peaks areas are observed for the pristine LiV_3O_8 sample at the different cycles. However, for the 2 wt.% ZnO-coated LiV_3O_8 sample, its differential capacity curves maintain original shapes and are almost overlapped at different cycles. In particular, the splitting of oxidation peak P'3 can not be observed, indicating that the electrochemical reversibility of 2 wt.% ZnO-coated LiV_3O_8 sample is very excellent.

According to the above results, we presume that three kinds of mechanism should be responsible for the improved electrochemical performance of 2 wt.% ZnO-coated LiV_3O_8 sample. One is that ZnO coating on the LiV_3O_8 cathode particles effectively suppresses the phase transitions during Li intercalation/deintercalation, which is reflected in Fig. 6(b) and consistent with the report in literature [27]. In addition, ZnO coating can prevent the dissolution of electrode materials considering the fact that vanadium-based oxides have the certain solubility in the organic electrolyte.

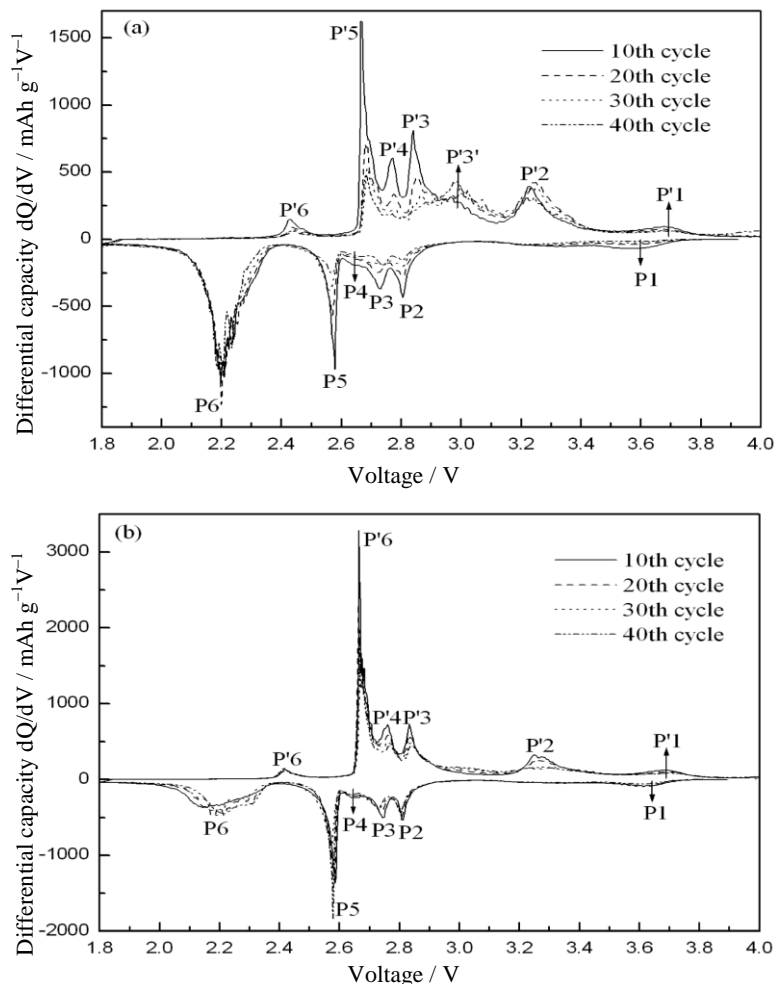


Figure 6. Differential capacity vs. voltage curves of (a) pristine LiV_3O_8 and (b) 2wt.% ZnO-coated LiV_3O_8 samples at different cycles

Last, ZnO-coated layer minimizes the harmful side reactions within the batteries by isolating the oxidizing cathode material and liquid electrolyte. These mechanisms together lead to an electrochemically synergistic effect that contributes to the excellent cycleability of 2 wt.% ZnO-coated LiV_3O_8 sample.

The cycling profile of the pristine LiV_3O_8 and 2 wt.% ZnO-coated LiV_3O_8 samples is presented in Fig. 7. It is found that the discharge capacity of the pristine LiV_3O_8 sample demonstrates serious fading during cycling and its capacity retention for the 44th cycle is only 61.38%. However, the 2 wt.% ZnO-coated LiV_3O_8 sample exhibits good cycling stability, keeping 87.86% of maximum capacity under same cycling condition. All of the above results show that the 2 wt.% ZnO-coated LiV_3O_8 exhibits a significant improvement in cycling stability, indicating that considerable improvement of the electrochemical properties of LiV_3O_8 by ZnO coating was feasible.

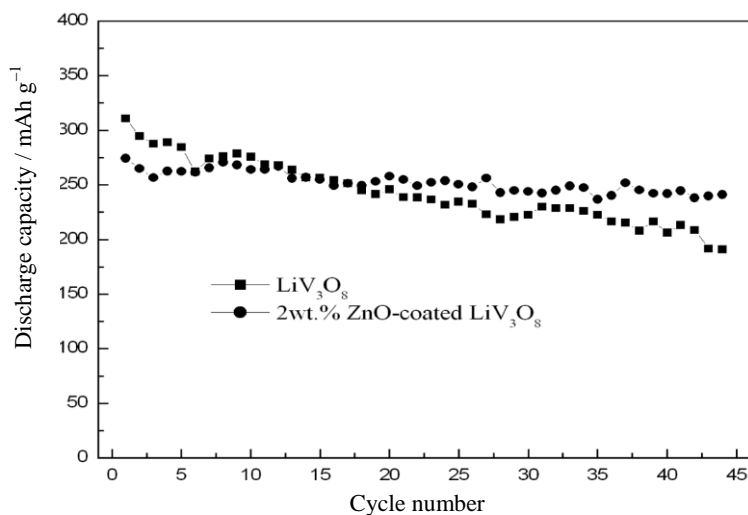


Figure 7. Long-term performance of pristine LiV₃O₈ and 2 wt.% ZnO-coated LiV₃O₈ sample

4. CONCLUSIONS

We have described a simple modified method to successfully synthesize the different weight ratios of ZnO-coated LiV₃O₈ samples. The results show that the ZnO is likely to be amorphous and coated on the surface of LiV₃O₈ samples. The surface modification with ZnO has been proved to be favorable to maintain a better cycling ability for LiV₃O₈. Among the different weight ratios of ZnO-coated LiV₃O₈ samples, the 2 wt.% ZnO-coated LiV₃O₈ sample demonstrates the first discharge capacity of 274.2 mAh g⁻¹ and stabilizes at 240.9 mAh g⁻¹ after 44 cycles, which is much higher than that of the pristine LiV₃O₈. In sum, the proposed modification technique with ZnO provides an alternative to ameliorating the cycleability of LiV₃O₈ material, which indicates the feasibility in improving electrochemical performance of LiV₃O₈ material by coating other electrochemically inactive oxides.

ACKNOWLEDGEMENT

This work was supported by the Young Core Teacher Program in Higher Education Institutions from the Education Commission of Henan Province, China (Grant No. 2009GGJS-059) and the Zhengzhou Municipal Science and Technology Development Programs, China (Grant No. 2010GYXM641).

References

1. H.Y. Xu, H. Wang, Z.Q. Song, Y.W. Wang, H. Yan, M. Yoshimura, *Electrochim. Acta* 49 (2004) 349.
2. Y. Zhou, H.F. Yue, X.Y. Zhang, X.Yu Deng, *Solid State Ionics* 179 (2008) 1763.
3. X. Cao, C. Yuan, X. Tang, L. Xie, X. Liu, H. Wang, X. Yan, *J. Iran. Chem. Soc.* 6 (2009) 698.
4. Y.C. Si, L.F. Jiao, H.T. Yuan, H.X. Li, Y.M. Wang, *J. Alloy. Compd.* 486 (2009) 400.

5. H.W. Liu, H.M. Yang, T. Huang, *Mater. Sci. Eng. B* 143 (2007) 60.
6. H. Yang, J. Li, X.G. Zhang, Y.L. Jin, *J. Mater. Process Tech.* 207 (2008) 265.
7. J.L. Sun, W.X. Peng, D.W. Song, Q.H. Wang, H.M. Du, L.F. Jiao, Y.C. Si, H.T. Yuan, *Mater. Chem. Phys.* 124 (2010) 248.
8. Y. Feng, F. Hou, Y. Li, *J. Power Sources* 192 (2009) 708.
9. X.L. Li, P.P. Li, M. Luo, X.Y. Chen, J.J. Chen, *J. Solid State Electrochem.* 14 (2010) 1325.
10. S.H. Ju, Y.C. Kang, *Electrochim. Acta* 55 (2010) 6088.
11. J.Q. Xu, H.L. Zhang, T. Zhang, Q.Y. Pan, Y.H. Gui, *J. Alloy. Compd.* 467 (2009) 327.
12. A.Sakunthala, M. V. Reddy, S. Selvasekarapandian, B. V. R. Chowdari, P. C. Selvin, *J. Phys. Chem. C* 114 (2010) 8099.
13. H.M. Liu, Y.G. Wang, K.X. Wang, Y.R. Wang, H.S. Zhou, *J. Power Sources* 192 (2009) 668.
14. V.R. Channu, R. Holze, E.H.W. Jr, S.A.W. Sr, R.R. Kalluru, Q.L. Williams, W. Walters, *Int. J. Electrochem. Sci.* 5 (2010) 1355.
15. A.D. Wadsley, *Acta Cryst.* 10 (1957) 261.
16. J.L. Sun, L.F. Jiao, H.T. Yuan, L. Liu, X. Wei, Y.L. Miao, L. Yang, Y.M. Wang, *J. Alloy Compd.* 472 (2009) 363.
17. L. Liu, L.F. Jiao, J.L. Sun, M. Zhao, Y.H. Zhang, H.T. Yuan, Y.M. Wang, *Solid State Ionics* 178 (2008) 1756.
18. L. Liu, L.F. Jiao, J.L. Sun, Y.H. Zhang, M. Zhao, H.T. Yuan, Y.M. Wang, *Electrochim. Acta* 53 (2008) 7321.
19. C.Q. Feng, L.F. Huang, Z.P. Guo, J.Z. Wang, H.K. Liu, *J. Power Sources* 174 (2007) 548.
20. M. Zhao, L.F. Jiao, H.T. Yuan, Y. Feng, M. Zhang, *Solid State Ionics* 178 (2007) 387.
21. L.F. Jiao, H.X. Li, H.T. Yuan, Y.M. Wang, *Mater. Lett.* 62 (2008) 3937.
22. X.Y. Cao, C. Yuan, L.L. Xie, H. Zhan, Y.H. Zhou, *Ionics* 16 (2010) 39.
23. Y. Feng, Y.L. Li, F. Hou, *Mater. Lett.* 63 (2009) 1338.
24. Y. Feng, Y.L. Li, F. Hou, *J. Power Sources* 187 (2009) 224.
25. Y.M. Liu, X.C. Zhou, Y.L. Guo, *Electrochim. Acta* 54 (2009) 3184.
26. L. Liu, L.F. Jiao, J.L. Sun, S.C. Liu, H.T. Yuan, Y.M. Wang, *Chin. J. Chem.* 27 (2009) 1093.
27. L.F. Jiao, L. Liu, J.L. Sun, L. Yang, Y.H. Zhang, H.T. Yuan, Y.M. Wang, X.D. Zhou, *J. Phys. Chem. C* 112 (2008) 18249.
28. S.H. Oh, S.M. Lee, W.I. Cho, B.W. Cho, *Electrochim. Acta* 51 (2006) 3637